Optimized Short-T_2 SNR and Resolution Using Ultrashort TE Imaging with T_2-Adapted Sampling

J. Rahmer[1], P. Börnert[1]

[1]Philips Research Laboratories, Hamburg, Germany

Introduction

Ultrashort echo-time imaging (UTE) employs 2D or 3D radial free-induction-decay (FID) sequences to minimize TE [1,2]. With echo times in the order of 100 µs and below, these techniques enable the detection of species with T_2 in the submillisecond range. However, choosing the optimal sampling window duration T_{AQ} for imaging short-T_2 components is not trivial. A short T_{AQ} reduces the overall signal-to-noise ratio (SNR), whereas a long T_{AQ} reduces resolution and SNR of short-T_2 components due to relaxation effects. To model T_2 relaxation effects, the point-spread function (PSF) was calculated for short-T_2 signal components acquired using the 2D or 3D UTE technique [3]. In this work, 3D UTE phantom measurements are presented to verify these simulations. Furthermore, an optimal T_{AQ} is derived, which maximizes SNR and resolution of short-T_2 signal components.

Methods

Figure 1 depicts a typical 3D UTE sequence. After a non-selective excitation pulse and a coil-dependent switching time in the order of 100 µs or less, the readout gradient is ramped up, and the acquisition of the FID is started. Thus, k space is mapped radially starting at $k = 0$. To ensure isotropic k-space coverage, projections are arranged with homogeneous angular spacing in 3D k space [4]. For 2D UTE, slice selective self-refocusing pulses are used in combination with 2D radial FID sampling [5].

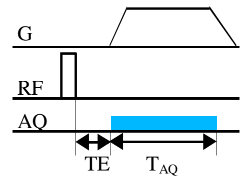

Figure 1: 3D ultrashort TE sequence applying a non-selective excitation pulse and FID sampling.

PSF simulations are shown in Fig. 2(a,b) for 3D and 2D radial FID sampling, respectively. T_2 decay during readout leads to centric signal decay in k space which causes PSF broadening and loss in amplitude. Simulations were done for different ratios between readout window duration T_{AQ} and T_2, under the assumption of a constant readout gradient. In the limiting case $T_{AQ} / T_2 \rightarrow 0$, the PSF in the absence of decay is obtained, i.e., a Sinc-like function in 3D and a "Jinc" in 2D (Fig. 2(a,b), solid lines) [3]. For $T_{AQ} / T_2 > 0$, the total PSF can be thought of as a convolution of the original PSF with a Lorentzian-type decay function. Total PSFs are shown for three exemplary T_{AQ} / T_2 ratios (Fig. 2(a,b), dashed lines). In Fig. 2(c), the T_{AQ} / T_2 dependence of the amplitude of the total PSFs is plotted in comparison with the amplitude of the decay functions only. Figure 2(d) shows the respective linewidths.

To verify these findings, 3D UTE phantom scans on a short-T_2 phantom with T_2 = 660 µs were performed on a clinical 3 T scanner (Achieva, Philips Medical Systems). Three scans at different readout window durations T_{AQ} = 0.68 ms, 3.50 ms, and 5.25 ms were performed. To extract the decay function from these scans, the short T_{AQ} image was deconvolved from the long T_{AQ} images using slight Wiener filtering to avoid singularities [6].

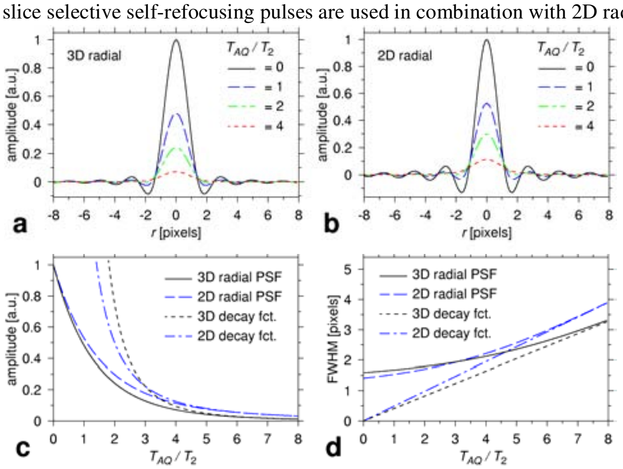

Figure 2: Radial PSF under the influence of T_2 decay. (a) Total PSF in case of 3D FID sampling for different ratios T_{AQ}/T_2. (b) Total PSF for 2D FID sampling. (c) Amplitude dependence of total PSFs and decay functions (cf. text) on T_{AQ}/T_2. (d) Linewidth dependence on T_{AQ}/T_2.

Results and Discussion

PSF simulations show a strong loss in amplitude and an increase in linewidth with increasing ratio T_{AQ} / T_2 (Fig. 2). While the amplitude loss is more pronounced for radial FID sampling in 3D than in 2D (Fig. 2(c)), the linewidth increase is less severe in 3D (Fig. 2(d)). The total PSF results from a convolution of the PSF in the absence of decay with a decay function. Extraction of the decay function from a series of phantom measurements (Fig. 3(a-c)) shows good agreement between experiment and simulation (Fig. 3(d)).

The above simulations suggest a ratio $T_{AQ} / T_2 \rightarrow 0$ to keep PSF amplitude high and blurring low. However, from sampling theory it follows that shortening the readout window decreases SNR with the square-root of the readout window duration. Thus, to find the optimal T_{AQ} for a given T_2, the PSF amplitude (cf. Fig.2(c)) has to be multiplied by the square root of T_{AQ} (cf. Fig. 4). This normalized single-voxel SNR has a maximum for a T_{AQ} / T_2 = 0.69 for 3D and 0.81 for 2D radial FID sampling. Comparison with Fig. 2(d) shows only a very slight linewidth increase for these T_{AQ} / T_2 ratios, namely 3.8 % for 3D and 7.1 % for 2D FID sampling. Consequently, not only a short TE is necessary to visualize short-T_2 components, but also a readout window duration T_{AQ} that is in the order of T_2. Otherwise, short-T_2 signal and resolution can be compromised. It will usually be necessary to apply high gradient strengths and slew rates to ensure sufficiently short readout windows.

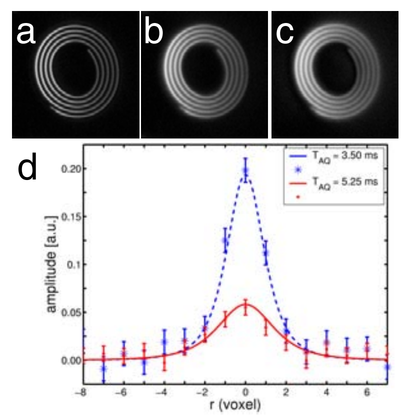

Figure 3: Phantom measurements and extracted blurring function. a) Short-T_2 phantom (T_2 = 660 µs) acquired with T_{AQ} = 0.68 ms. (b) T_{AQ} = 3.50 ms. (c) T_{AQ} = 5.25 ms. (d) Blurring functions (asterisks, dots) obtained from a deconvolution of image (a) from (b) and (c), respectively. The curves represent the simulated decay functions for the respective T_{AQ} / T_2 ratios.

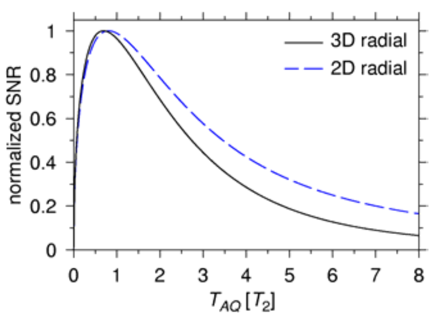

Figure 4: Single voxel SNR obtained from the PSF amplitude (cf. Fig. 2(c)) weighted with the square-root of the sampling window duration T_{AQ}. The functions have a maximum at T_{AQ} = 0.69 T_2 for 3D and 0.81 T_2 for 2D sampling.

Conclusion

Calculation of the PSF for 3D radial FID sampling under the influence of T_2 decay exhibits increasing loss in short-T_2 SNR and resolution with increasing sampling window duration T_{AQ}. On the other hand, a short T_{AQ} reduces overall SNR. An optimum can be found which maximizes SNR for short-T_2 components with negligible loss in resolution. If T_2 of the species to be imaged is known, UTE scans should apply the corresponding ideal readout duration for optimal results.

References

[1] Gatehouse PD *et al.*, Clin. Radiol. **58**, 1-19 (2003).
[2] Glover GH *et al.*, J. Magn. Reson. **2**, 47-52 (1992).
[3] Rahmer J *et al.*, Proc. ISMRM **13**, 2354 (2005).
[4] Wong S *et al.*, Magn. Reson. Med. **32**, 778-784 (1994).
[5] Pauly JM *et al.*, Proc. SMR **8**, 28 (1989).
[6] Press WH *et al.*, Num. Rec. in C, Cambridge (1992).